Sensors & Transducers, Vol. 237, Issue 9-10, September-October 2019, pp. 43-51

www.sensorsportal.com

Sensors & Transducers

Published by IFSA Publishing, S. L., 2019
http://www.sensorsportal.com

Micro-structured Optical Spectrometer Sensor in PMMA

[1, *] Fischer-Hirchert Ulrich H. P., [2] Höll Sebastian, [1] Haupt Matthias and [3] Joncic Mladen

[1] Harz University of Applied Sciences, Friedrichstr. 57, 38855 Wernigerode, Germany
[2] Sicoya GmbH, Carl-Scheele-Straße 16, 12489 Berlin, Germany
[3] IAV GmbH, Carnotstraße 1, 10587 Berlin
Tel.: + 49 3943659 351, fax: + 49 3943659 5351
E-mail: ufischerhirchert@hs-harz.de

Received: 30 August 2019 /Accepted: 27 September 2019 /Published: 30 November 2019

Abstract: Data communication over Polymer Optical Fibers (POF) is limited to only one channel for data transmission. Therefore the bandwidth is strongly restricted. By using more than one channel, it is possible to break through the limit. This technique is called Wavelength Division Multiplexing (WDM). It uses different wavelengths in the visible spectrum to transmit data parallel over one fiber. Two components are essential for this technology: A multiplexer (MUX) and a demultiplexer (DEMUX). The multiplexer collects the light of the different sources to one fiber and the demultiplexer separates the light at the end of the fiber into the different fiber output ports. In this paper, we show the realization of a grating spectrometer realised by injection moulding in PMMA, working in the visible spectrum, respectively. We present the results of a demonstrator of an integrated polymeric spectrometer device produced with injection moulding in combination with hot embossing. The paper discusses the results of the different development steps, the measurements done with the first demonstrator and the challenges related to the injection moulding process.

Keywords: Optical spectrum analyzer, PMMA injection moulded optical spectrum sensor, Hot embossing sensor, Polymeric fiber WDM systems, POF over WDM.

1. Introduction

Polymer Optical Fibers (POF) are used in various fields of applications. The core material consists of PMMA (Polymethylmethacrylate), while the cover is made of fluorinated PMMA. The whole fiber has a diameter of 1 mm. POFs are used for optical data transmission based on the same principle as glass fiber. As a communication medium they offer a couple of advantages related to other data communication systems such as copper cables, glass fibers and wireless systems, and have great potential to replace them in different applications.

Namely, in comparison with glass fibres (GOF), POFs have the advantage of easy and economical processing and are more flexible for optical connections [1]. However, one advantage of using glass fibres is their low attenuation, which is below 0.2 dB/km in the infrared range. The larger core diameter of POFs leads to higher mode dispersion and thus to higher attenuation across the electromagnetic spectrum. This increased attenuation leaves only one remaining transmission window, namely the visible spectrum of light (400 – 700 nm). Hence, POFs are best suited for the use in short distance data communication.

Here, POFs can outperform the current standard of copper cable as communication medium. On the one hand, they feature lower weight and space. On the other hand, POFs are not susceptible to

electromagnetic interference [2-3]. For these reasons, POFs are already used in various application domains, for example in the automotive sector and for in-house communication [4-7]. At present, the great potential of the POF is not available as the alternative techniques offer transmission rates up to 10 Gb over copper and up to 40 Gb over glass fibers in the network area. The WDM technique offers an approach to achieve these high data rates also in the POF range.

For WDM two essential components are needed: a multiplexer and a demultiplexer. To create a functional demultiplexer for POF, several preconditions must be fulfilled. Firstly, a mirror must focus the divergent light beam coming from the POF. The shape of this mirror cannot be spherical because of the appearing spherical aberration. Instead, a toric shape of the mirror prevents spherical aberration [8-10].

The second function is the separation of the different transmitted wavelengths, which can be achieved by a diffraction grating. This principle is illustrated in Fig. 1. The light is split into different orders of diffraction. The first order is the important one to regain all information. There, the outgoing POFs can be placed.

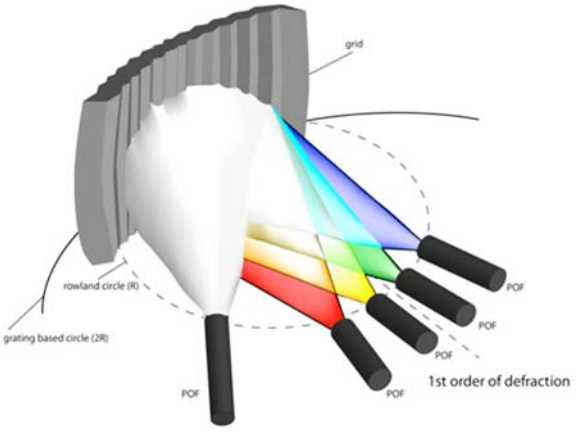

Fig. 1. Rowland set-up of integrated PMMA spectrometer.

To separate the channels at the output ports, one interesting option for high multimode transmission systems is to use an optical grating. Here, the optical grating is placed on an aspheric mirror, which focuses the monochromatic parts of light into the outgoing fibers. In order to keep the advantage of cost-effective POFs it is necessary to mass-produce the MUX and DEMUX component at reasonable prices. For polymers, injection molding is the only technology, which offers high potential to achieve this goal.

As explained, a concave diffraction grating was used to develop the DEMUX. This section details the optical grating and its properties.

The diffraction on a lattice can be clearly described with Fig. 2. The figure shows an incident light beam with the angle θi to the lattice normal, which is diffracted at the lattice at the angle θ_m. The index m stands for the diffraction order. Fig. 2 shows a reflective grid structure with a grid line distance d. Looking at the second light beam, which is diffracted at the adjacent grid line, it creates a path difference of $d\sin\theta_m$ - $d\sin\theta_i$ between the two beams. If this path difference is equal to or an integer multiple of the wavelength of the incident light, then the constructive interference of the two neighboring rays occurs [16]. This is the basis for the preparation of the grid equation, which calculates as follows [13].

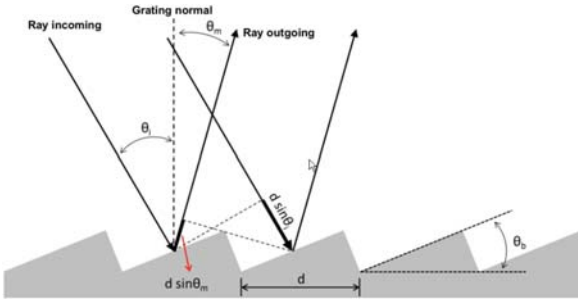

Fig. 2. Schematic representation of the diffraction angles on a reactive blazed lattice.

$$m\lambda = d\,(\sin\theta_m - \sin\theta_i), \tag{1}$$

$$\sin\theta_m = \sin\theta_i \frac{m\lambda}{d} \tag{2}$$

where m is the diffraction order, θ_t is the angle of incidence of the light and θ_m is the angle of reflection of the diffracted light.

Converted according to the angle of incidence of the diffracted light beams in the different diffraction orders, Eq. (2) gives the following equation:

$$\theta_m = \arcsin\left(\sin\theta_i + \frac{m\lambda}{d}\right) \tag{3}$$

Another peculiarity of the lattice structure can be seen in Fig. 2. The lattice structure consist of saw teeth whose flanks have an angle θ_b to the lattice base. This arrangement is called blaze condition and the angle θ_b blaze angle [16]. Normally, the intensity of the light diffracted at the grating is distributed over all diffraction orders. With the blazed grating it is possible to divert a large part of the energy into a certain order of diffraction. The blaze condition can be expressed as follows [16]:

$$m\lambda = 2d\sin\theta_b \tag{4}$$

With a defined blaze angle and a defined diffraction order the so-called blaze wavelength can be calculated, in which the lattice efficiency reaches its maximum. While it is relatively easy to determine the blaze wavelength, it is much more complex to compute the maximum efficiency value. This calculation is generally performed via simulation

programs (e.g., OpTaliX) and simulates the course of lattice efficiency in a selected wavelength range. Since the transmission window is in the wavelength range of 400 - 700 nm, it is expedient to place the blaze wavelength approximately in the middle. The best lattice over the wavelength range can be achieved with λ_b = 518.5 nm. The course of the effectivity and the simulation results of the grid are summarized in [23-24]. With the blaze wavelength being in the second diffraction order, the blaze angle can be calculated to be $\theta_b = 11.97°$.

A very important parameter for the properties of the DEMUX is the angular dispersion. For a fixed angle of incidence qi this means the change of the angle θ_m as a function of the wavelength λ of the incident light, i.e. the quantity $\partial\theta_m/\partial\lambda$.

The greater the angular dispersion, the stronger the spectral splitting, the further apart the interference maxima for light waves of different wavelengths are. A large angular dispersion is a prerequisite for a large spectral resolution. By deriving the lattice Eq. (2) by the wavelength and at a constant angle of incidence qi, the angle dispersion results to [13]:

$$\frac{\partial\theta_m}{\partial\lambda} = \frac{m}{d\cos\theta_m}\left[\frac{\partial\theta_m}{\partial\lambda}\right] = \frac{Grad}{m} = 10^{-9}\frac{Grad}{nm} \qquad (5)$$

Since the DEMUX is a component made of transparent plastic, the light from the POF is completely guided in the material of the DEMUX. Consequently, there is no transition from PMMA (core of the POF) to air. First, this results in the Numerical Aperture (NA) of the fiber being reduced to e.g. PMMA to PMMA-DEMUX: NA = 0.34. Second, the wavelength of the light, when it enters another medium (other than air or vacuum), changes to:

$$\lambda M = \lambda / n_M(\lambda) \qquad (6)$$

where λ_M is the wavelength of the light in the medium, λ is the wavelength of the light in the vacuum and $n_M(\lambda)$ is the wavelength-dependent refractive index of the medium. It can be seen that with a refractive index > 1 the wavelength shortens. This must be taken into account when considering the grid equation for the wavelengths to be transmitted.

2. Production Method for Concave Lattice Structures

2.1. Micromechanical Fabrication Methods

As emerged from the previous sections, a 3-dimensional approach to the DEMUX element must be determined. The challenge is to fabricate the device with a concave, 3-dimensional, micro structured diffraction grating, which also has the function of positioning and combining the input and output fibers. This includes photolithographic production methods and LIGA (acronym for lithography, electroplating and impression taking) [17], which are largely established in the manufacture of MEMS components (micro-electro-mechanical systems), but for the production of the DEMUX unsuitable. Although these are characterized by smaller structure sizes and the high production rate due to batch processes. Unfortunately, they are limited to planar component geometries with a maximum of 2.5 dimensions.

On the other hand, mechanical micromachining brings many advantages in terms of making the DEMUX. Among other things, these include the creation of complex geometries, higher relative accuracies and greater freedom in the choice of component material. A comparison between MEMS-based manufacturing methods and mechanical micromachining is shown in Table 1.

Table 1. Comparison between MEMS processes and micromachining processes

	MEMS process	**Micromachining**
Edit. material	Silicon, some metals	Metals, alloys, plastics, ceramics, glasses
Component geometry	Planar to 2.5D	3D
Rel. accuracy	10^{-1} - 10^{-3}	10^{-3} - 10^{-5}
Process control	Feedforward	Feedback
Production volume	High	High or low
Production rate	High	Small
Total investment	High	Medium to small
Applications	MEMS, microelectronics planar microcomponents	Various 3D microcomponents

Furthermore, the methods of micromachining can be classified according to their underlying mechanisms. It differs physical, chemical and mechanical removal mechanisms. The mechanical processes are divided into cutting and abrasive methods.

These are subdivided into grinding and polishing for the abrasives and diamond turning and diamond milling in the area of cutting processes. Diamond turning and milling are known as ultra-precision machining. This technique is discussed in more detail in the next section.

2.2. Ultra-precision Machining

Ultra-Precision Machining (UPB) is a machining with a diamond tool. Only a very small layer of the surface is removed, but this with the highest precision. Ultra-precision machining is one of the most important techniques for producing high-precision

components with surface roughnesses of a few nanometers (1-10 nm) and tolerance deviations in the sub-micron range. Spherical and aspherical surfaces can be produced with high optical quality. [19-20] Optical precision can only be achieved by using extremely high-precision mechanical positioning systems become. Today's systems achieve exceptionally high mechanical precision and stability [19].

Before starting the production of the mold insert, a demonstrator of the DEMUX is fabricated by directly machining it in the PMMA material by means of diamond turning technique (see Fig. 3). Thus, the same diamond-turning technology is used for the manufacture of the mold insert. This step is done due to validate the simulation results with the produced component.

The UPB offers several advantages when creating the optical DEMUX:

- Real 3D structure creation;
- Production of optical surfaces up to the edge of the element with roughness in the single-digit nanometer range;
- Components with variable aspect ratios can be realized;
- Machining soft ductile materials which are difficult to polish;
- Possibility to integrate adjustment elements;
- Production of forms, which are difficult to reach with other methods.

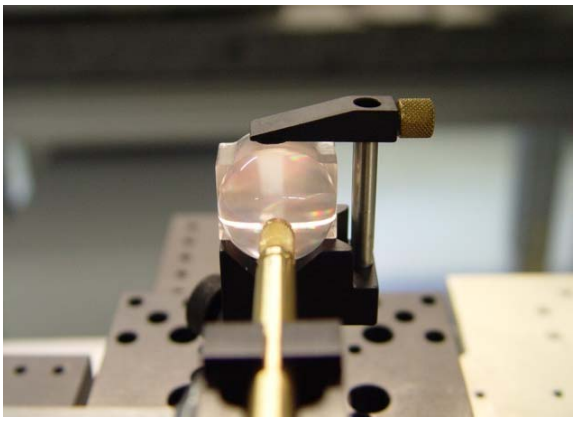

Fig. 3. Prototype of integrated PMMA spectrometer.

UPB is often used for the prototype production of PMMA lens surfaces. Experimental results show that during processing of PMMA, there is little variation in dynamic cutting force and continuous chip formation. This is very beneficial for the machining of micro and nanostructures. The amorphous and ductile nature of PMMA makes it possible to directly cut optically qualitative surfaces without any post-processing.

For this reason, it is not possible, according to the state of the art, to use UPB directly to produce hardened steel injection molds, which is the preferred material for producing tools. The production therefore takes place in two steps. The first step is to create a structure in steel that approximates the natal structure. Then a thin Layer (up to 500 mm) nickel chemically (electroless) deposited on the steel surface. In the second step, the male structure is introduced into the nickel layer by means of UPB. In this way, the resistance to the high pressures during injection molding (sometimes more than 1000 bar [22]) can be greatly increased. [21].

3. Manufacturing of the Demonstrator

The selection of a suitable material for the production of an optical system depends on various criteria:

- Optical properties;
- Mechanical properties;
- Thermal and thermomechanical properties;
- Resistance to environmental influences;
- Availability and costs.

That all these features are considered in one application is rare. Typically, different applications only require the evaluation of one to two criteria. For example, transmissive components are chosen for their optical properties, while reactive components are distinguished by their mechanical and thermal properties. Materials used for the injection molding of optical components must meet high thermal requirements and be resistant to external environments (e.g., high pressure).

The number of materials that can be processed with UPB is increasing continuously. An excerpt from the most important workable materials is the following list:

- Aluminum alloys (1100, 2011, 2017, 2024, 3003, 5086, 5186, 6061, 7075);
- Brass;
- Copper (OFHC-Oxygen free high conductivity copper, galvanic copper, Alloys with beryllium);
- Gold;
- Nickel (chemically with 10-12% phosphorus content);
- Silver;
- Tin;
- Zinc;
- Polymethylmetacylate (PMMA);
- Polycarbonate (PC).

Not all of these materials are equally well suited for diamond machining. Optimum manufacturing parameters (e.g., rotational speeds and feed, coolant, and tool condition) are very different for each material. Some of these materials are preferred in terms of the ability to produce optically smooth and geometry-stable surfaces with the UPB. Among the metals are: aluminum, copper, galvanic copper and chemical nickel.

PMMA is the best material to process among the polymers.

By using the injection molding process, the manufacturing of the mold insert is the most important factor. Due to the three-dimensional toric structure of the grating planar manufacturing methods like

lithography, especially LIGA cannot be used. LIGA is used to manufacture planar spectrometers based on the glass fiber technology [11-14]. But in our case, the three-dimensional grating needs another machining method. Especially the microstructure of the grating and the exact curve shape of the toric surface require high precision.

The microstructure has the shape of a saw tooth with a pitch between the teeth of 2.5 µm. Fig. 4 shows an enlarged 3D-Model of the grating. After investigate several machining methods only the diamond turning meets the high demands of the micro structured grating.

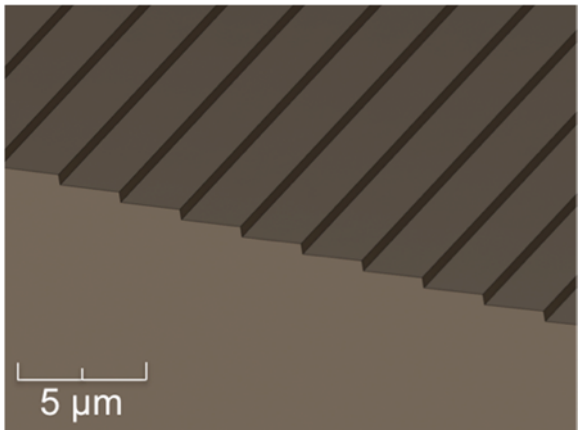

Fig. 4. 3D Sawtooth like simulation of the grating of the prototype.

4. Transmission Measurements

Prior to the production of the DEMUX some preliminary investigations have taken place to find the best suitable material for the demultiplexer. Therefore, both the processability of the material and the optical parameters had to be considered in detail. The injection molding process was tested with a thick-walled mold (see Fig. 5).

This test tool had the same shape as the final DEMUX, except for the grid. The test runs were carried out with an injection-molding machine from Babyplast 6-10P. This device was able to inject precisely small parts. Table 2 lists all the materials used for the study. Further parameters such as the respective melt volume rate (MVR) and light transmittance (according to the manufacturer's specification) are depicted. The test was additionally used to find the optimized injection molding process parameters for the material.

In addition, the optical quality of the polymer materials must be investigated. Therefore, a mold for injection molding test plates was designed. The test plates had a thickness of 2 mm. The mold is used to make samples from each material listed in Table 2. The DIN EN ISO 13468-2 standard describes the measurement of the optical transmission of polymer materials. Therefore, the test plates are designed to meet this standard.

Transmission measurements were carried out with all test plates. The results are shown for 405 nm in Fig. 6. It can be seen that both ZEONEX types and PMMA POQ62 show the highest value for the light transmission. PMMA POQ62 is a polymer grade with high purity of polymer granulates. The measurement is made at a wavelength of 405 nm because it is one of the wavelengths used for the WDM system. [18].

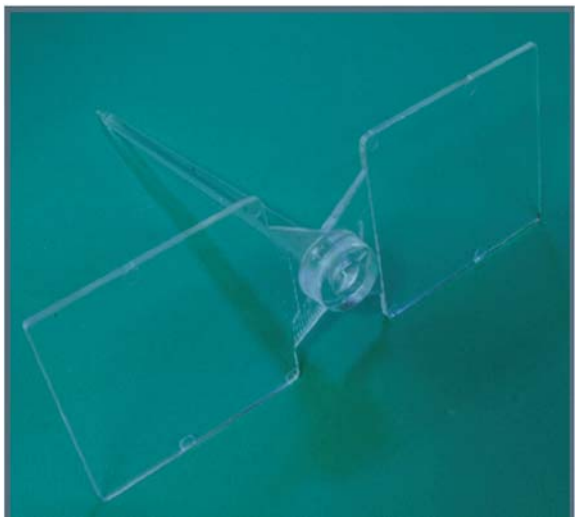

Fig. 5. Molded part of the sample plates made of PMMA.

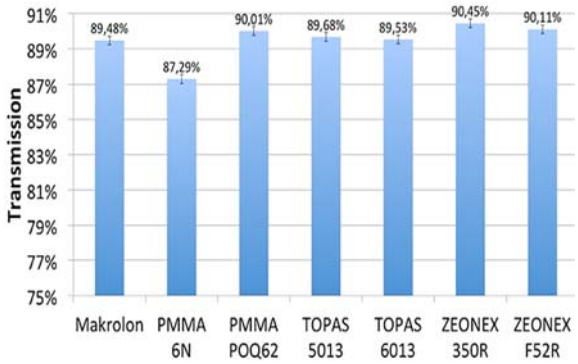

Fig. 6. Transmission of different material at 405 nm.

Table 2. Injection molding materials for the integrated spectrometer element.

Name	Type	MVR [cm³/10min]	Transmission [%]
Plexiglas 6N	PMMA	12	92
Plexiglas POQ62	PMMA	21	92
Topas 5013L-10	COC	48	91.4
Topas 6013M-07	COC	14	91
ZEONEX F52R	COP	22	92
ZEONEX 350R	COP	26	92
Makrolon LED2245	PC	35	90

5. Demonstrator Characterization

In order to verify the function of the spectrometer prototype and to compare it with the simulation results, a high-precision measuring setup has to be realized.

As is known from Chapter 3, the prototype consists of the lattice structure and a hemisphere located on the Rowland circle. Centric on this hemisphere, the polymer fiber is adjusted to couple in the light. With a second POF, the hemisphere is scanned to determine the position of the maxima of the different wavelengths. Fig. 7 shows the measuring arrangement as a CAD model.

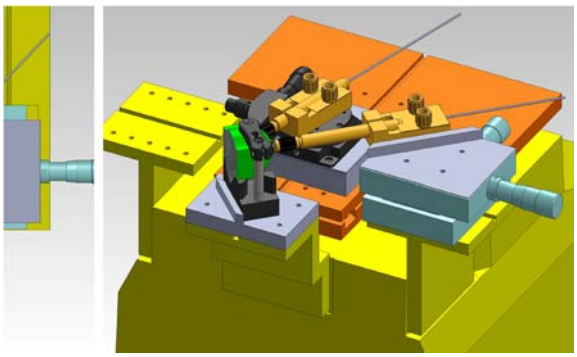

Fig. 7. Test setup for determining the functionality of the DEMUX prototype.

To increase the coupling efficiency during the scanning process, index matching gel is applied between the scanning fiber and the hemisphere surface. The index matching gel replaces the air gap between the two optical surfaces (DEMUX and POF) by a medium having the same refractive index as the polymer fiber. Thus, Fresnel losses are avoided.

The positioning system used was the F-206 6-axis adjustment system from Physik Instrumente (PI) with an aperture of 0.1 µm or 2 µrad. Thus, an accurate sampling can be performed with the output POF. In order to position the starting POF always perpendicular to the hemisphere surface for scanning, the holder for the original POF was mounted on an additional rotation table. This is to ensure that occurring losses are minimized by tilting the fiber to the exit plane of the light. The complete setup can be seen in Fig. 8.

Fig. 8 shows the principle of the measurement. The input fiber is fixed on the center of the Roland circle. The output fiber is moved along the Rowland rice and always points towards the grid center. The DEMUX is at an angle of 45° to the normal of the PI system, as shown in Fig. 8. When scanning the Rowland circle, the angle of the fiber (which is set via the turntable) changes in relation to the grating center. The output fiber touches the point C the Rowland circle. This results in two coordinate systems. Once the coordinate system of the DEMUX and the coordinate system of the PI positioning system. In order to determine the coordinates of the point C in the PI coordinate system, a coordinate transformation must be performed.

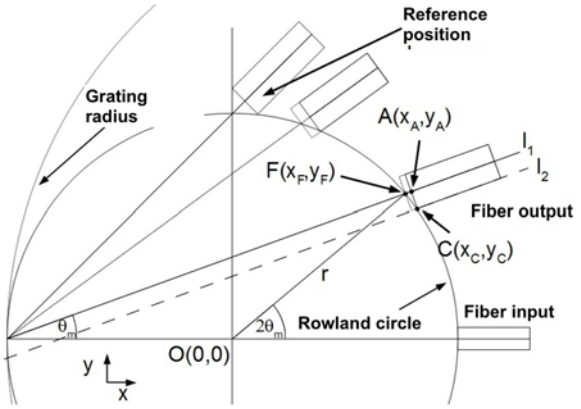

Fig. 8. Schematic representation of the characterization measurement method, in which the output fiber points towards the center of the grating.

The following quantities must be determined for the system to perform the transformation:

- Distance of the fiber end face to the fulcrum;
- Radius of the Rowland circle ($r_{rowland}$=11.25 mm);
- Coordinates of the reference point in the PI coordinate system.

First, the reference position is approached under a microscope. This is the basis for calculating the coordinates of the output fiber. The coordinate transformations are then performed.

1 Transverse shift around the vector ($r_{rowland}$= 0): This moves the zero point to the center of the Rowland circle.

2 Rotation by 45 ° using rotation matrix: rotation around 45 ° center of the Rowland circle.

3 Transverse shift around the reference point: Shift of the coordinate system by the PI coordinates of the reference point, which was previously determined by approaching the reference point with the PI system.

4 Correction of the fiber displacement by rotation of the turntable: By the rotation of the fiber, the fiber front facet shifts due to the distance to the fulcrum. The result is the coordinates for the point A.

5 Parallel shift around the vector (0; 0; 5): this shift describes the offset between point A and point C by half the fiber diameter.

An exact derivation of the coordinate transformations is described in [23-24]. With the coordinates of the fibers as a function of the diffraction angle, the surface can be scanned. For the measurement, a resolution of 0.5 ° can be achieved due to the turntable.

In Fig. 9 can be seen that the separated wavelength are focused at a ring on the hemisphere. This ring is scanned by the fiber on the alignment system. The light of the scanning fiber is analyzed by a spectrometer. The positions of the wavelengths measured are depicted also in Fig. 9. In comparison to

the simulation a shift of the positions can be recognized. Nevertheless, the separation of the wavelengths was measured and confirms the functionality of the demultiplexer.

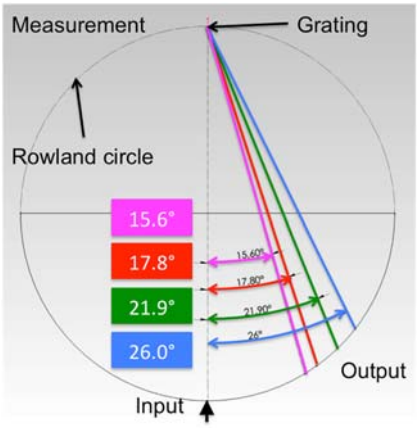

Fig. 9. Measurement results of the focal points for different wavelengths (405 nm violet ray; 450 nm blue ray; 520 nm green ray; 650 nm red ray.

6. Manufacturing of the Demonstrator

By using the injection molding process, the manufacturing of the mold insert is the most important factor. Due to the three-dimensional toric structure of the grating planar manufacturing methods like lithography, especially LIGA cannot be used [14].

The microstructure has the shape of a sawtooth with a distance between the teeth of 2.5 µm. Fig. 4 shows an enlarged 3D model of the grating. An in-depth investigation of various processing methods has shown that only the diamond turning fulfills the high requirements of the production of the microstructural lattice. The diamond twisting technique is a special machining method using a single crystal diamond-cutting tool. It is also possible to produce a surface with an optical quality at the edge of the optical component. It offers several advantages:

- True three-dimensional contour generation;
- Accuracy of one part in 106 with absolute accuracy of 1 part in 108 on a single axis for ideal conditions;
- Surface finish of 5 nm Ra for a range of materials and as good as 1 nm Rz;
- Ability to generate surfaces with variable aspect ratios, and
- Feature sizes that exceed the limits of optical microscopy [11-14].

A metallization process was used to analyze the surface of the lattice. The surface was sputtered with a thin aluminum layer depicted in Fig. 10. It is now possible to measure the shape of the surface with a white light interferometer and to examine the lattice structure under the scanning electron microscope (SEM).

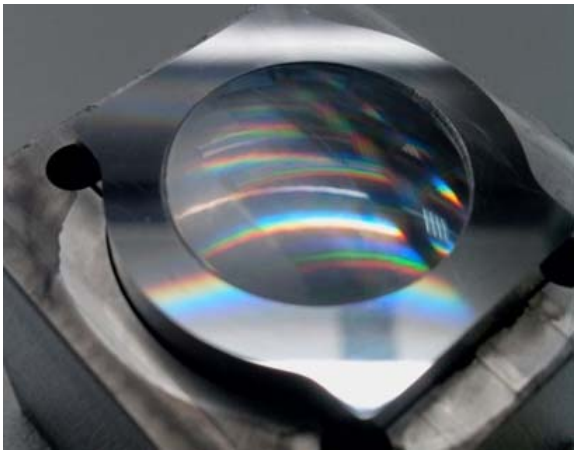

Fig. 10. High quality structures of the grating.

The metallized surface of the grating is shown in Fig. 10. It can be seen that the structure on the left side has a dull and mat surface instead of the glossy residue of the surface. This is a first indication that the surface roughness in this part is higher and does not meet the requirements for the component precision. The first visual impression was then confirmed by the analysis under the SEM which is depicted in Fig. 11.

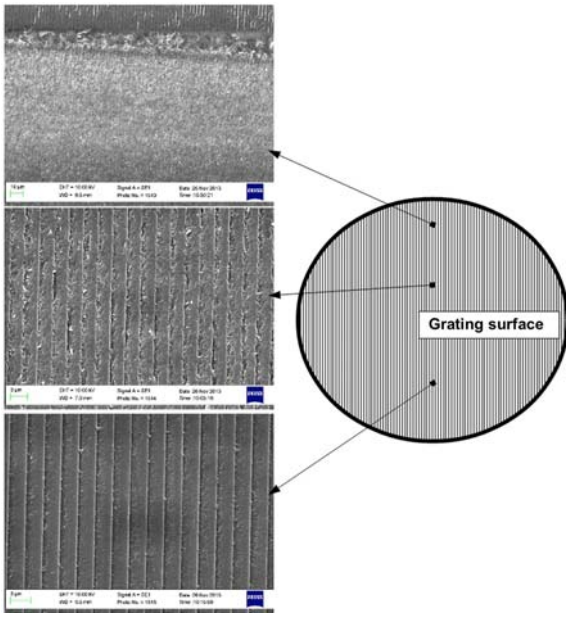

Fig. 11. SEM photographs of the structures of the grating at different locations.

The grid quality is excellent in the first half of the grid. From half of the quality deteriorates and ultimately merges into the dull, unstructured area at the edge. Above all, however, the grid line spacing, as in Table 3, is within the required tolerance.

On the other hand, improvements in the area of the radii of the grid and the grid height still have to be made. As shown in Table 3, these are still too low. Furthermore, the packaging and handling of the

DEMUX has to be improved, since there are small scratches on the grid surface.

Table 3. Summary of the measurement results.

Parameter	Measured value	Desired value	Dev. [%]	Impact
Radius in x r_x	20.128 mm	20.3 mm ±0.01 mm	-0.85	Focus point magnification, aberrations
Radius in y r_y	22.314 mm	22.5 mm ±0.01 mm	-0.83	Focus point magnification, aberrations
Grid height h_{Gitter}	1.847 mm	1.878 mm ±0.01 mm	-0.83	Expansion of focal points
Grating line spacing d	2.55 µm	2.5 µm ±0.1 µm	+2.00	Shift of Diffraction angle and blaze angle

7. Conclusions

In summary, injection moulding the spectrometer element for POFs poses several challenges, especially the microstructure of the grating on a three-dimensional surface. It is shown that the current manufacturing process is able to produce the structure size and the exact radius needed for the spectrometer used as a DEMUX for POF over WDM. The optical measurements to prove the principle were done. These confirm the separation of the wavelength in the visible spectrum.

The device is also a very good candidate for optical sensor applications. The component can be used both in the registration of paint colors of the automotive industry or paint industry, as well as in the recognition of the textile inks in the textile industry. Furthermore, there is the possibility of measuring residual proportions in the waste water of dishwashers for dosing of rinse water and detergent.

Acknowledgements

We gratefully acknowledge the funding by the German Ministry of Education and Research (BMBF) under grant number 16V0009 (HS Harz) / 16V0010 (TU BS). All injection moulded parts are done with the support of the Institute of Micro and Sensor Systems at the Otto-von-Guericke University Magdeburg and Prof. Bertram Schmidt.

References

[1]. W. Daum, J. Krauser, P. E. Zamzow, O. Ziemann, POF Handbook: Optical Short Range Transmission Systems, *Springer-Verlag*, 2008.

[2]. H. S. Nalwa (Ed.), Polymer Optical Fibres, *American Scientific Publishers*, California 2004.

[3]. Club des Fibres Optiques Plastiques (CFOP) France, in Plastic Optical Fibres – Practical Applications, (J. Marcou, Ed.), *John Wiley & Sons*, Masson, 1997.

[4]. J. Brandrup, E. H. Immergut, E. A. Grulke, Polymer Handbook, 4th Edition, *Wiley-Interscience*, 1999.

[5]. R. T. Chen, G. F. Lipscomb, Eds., WDM and Photonic Switching Devices for Network Applications, in *Proceedings of the SPIE*, Vol. 3949, 2000.

[6]. Colachino J., Mux/DeMux Optical Specifications and Measurements, *Lightchip Inc. White Paper, Lightreading*, 2001.

[7]. A. H. Gnauck, A. R. Chraplyvy, R. W. Tkach, J. L. Zyskind, J. W. Sulhoff, A. J. Lucero, *et. al*., One terabit/s transmission experiment, in *Proceedings of the OFC'96*, 1996.

[8]. Fischer-Hirchert U. H. P., Photonic packaging sourcebook: Fiber-chip coupling for optical components, basic calculations, modules, *Springer-Verlag,* 2015.

[9]. U. H. P. Fischer-Hirchert, M. Haupt, WDM over POF: the inexpensive way to breakthrough the limitation of bandwidth of standard POF communication, in *Proceedings of the SPIE Symposium on Integrated Optoelectronic Devices*, *Photonics West*, San Jose, 2007.

[10]. U. H. P. Fischer-Hirchert, M. Haupt, Integrated WDM System for POF Communication with Low Cost Injection Moulded Key Components, *Access Networks and In-house Communications*, 2010.

[11]. M. Stricker, G. Pillwein, J. Giessauf, Focus on Precision - Injection Molding Optical Components, *Kunststoffe International*, Vol. 4, 2009, pp. 15-19.

[12]. J. P. Ferguson, S. Schoenfelder, Micromoulded spectrometers produced by the Liga Process, in *Proceedings of the IEE Two-day Seminar Searching for Information: Artificial Intelligence and Information Retrieval Approaches, (Ref. No. 1999/199)*, 1999, pp. 11/1-11/4.

[13]. M. A. Davies, C. J. Evans, R. R. Vohra, B. C. Bergner, S. R. Patterson, Application of precision diamond machining to the manufacture of microphotonics components, in *Proceedings of the SPIE 5183, Lithographic and Micromachining Techniques for Optical Component Fabrication II, 94*, November 2003.

[14]. D. Dornfeld, S. Min, Y. Takeuchi, Recent Advances in Mechanical Micromachining, *CIRP Annals - Manufacturing Technology*, Vol. 55, Issue 2, 2006, pp. 745-768.
www.nwlab.net/know-how/JPerf/, Website 1.9.2017

[15] E. G. Loewen, E. Popov, Diffraction Gratings and Applications, *Marcel Dekker, Inc.*, 1997

[16]. C. Palmer, Diffraction Grating Handbook, Vol. 46, *Newport Corporation*, 2005.

[17]. A. Last, Fehllicht in LIGA-Mikrospektrometern, *Dissertation Universität Karlsruhe*, 2002

[18]. U. H. P. Fischer-Hirchert, *et al*., Optical sensor systems with micro-structured grating in PMMA for POF-applications, in *Proceedings of the 5th International Conference on Sensors and Electronic Instrumentation Advances (SEIA'19)*, Adeje, Tenerife (Canary Islands), Spain, 25-27 September 2019, pp. 9-12.

[19]. W. B. Lee, B. C. F. Cheung, Surface Generation in Ultraprecision Diamond Turning: Modelling and Practices, *Wiley*, 2002

[20]. E. Brinksmeier, W. Preuss, Micro-machining, in Philosophical Transactions: Mathematical, Physical and Engineering Sciences, *Royal Society,* Vol. 370, Issue 1973, Aug 2012, pp. 3973-3992.

[21]. S. Bäumer, T. Bauer, D. Marschall, Handbook of Plastic Optics, *Wiley-VCH Verlag*, 2010

[22]. R. Mayer, Precision Injection Molding, *Optik & Photonik*, Vol. 2, Issue 4, 2007

[23]. M. Haupt, U. H. P. Fischer-Hirchert, Optical design of a low-loss demultiplexer for optical communication systems in the visible range, *SPIE Optical Systems Design*, Vol. 8550, 2012, 85500J.

[24]. S. Höll, Herstellung eines Wavelength Division Multiplex (WDM) Demultiplexer für Optische Polymerfasern (POF)m im Spritzgussverfahren, *Cuvillier Verlag Göttingen*, 2018
